Efficient bone cutting with the novel diode pumped Er:YAG laser system: in vitro investigation and optimization of the treatment parameters

Karl Stock, Rolf Diebolder, Florian Hausladen, Raimund Hibst
Institut für Lasertechnologien in der Medizin und Meßtechnik an der Universität Ulm,
Helmholtzstraße 12, 89081 Ulm, Germany

ABSTRACT

It is well known that flashlamp pumped Er:YAG lasers allow efficient bone ablation due to strong absorption at 3µm by water. Preliminary experiments revealed also a newly developed diode pumped Er:YAG laser system (Pantec Engineering AG) to be an efficient tool for use for bone surgery.

The aim of the present in vitro study is the investigation of a new power increased version of the laser system with higher pulse energy and optimization of the treatment set-up to get high cutting quality, efficiency, and ablation depth.

Optical simulations were performed to achieve various focus diameters and homogeneous beam profile. An appropriate experimental set-up with two different focusing units, a computer controlled linear stage with sample holder, and a shutter unit was realized. By this we are able to move the sample (slices of pig bone) with a defined velocity during the irradiation. Cutting was performed under appropriate water spray by moving the sample back and forth. After each path the ablation depth was measured and the focal plane was tracked to the actual bottom of the groove. Finally, the cuts were analyzed by light microcopy regarding the ablation quality and geometry, and thermal effects.

In summary, the results show that with carefully adapted irradiation parameters narrow and deep cuts (ablation depth > 6mm, aspect ratio approx. 20) are possible without carbonization.

In conclusion, these in vitro investigations demonstrate that high efficient bone cutting is possible with the diode pumped Er:YAG laser system using appropriate treatment set-up and parameters.

Keywords: Er:YAG laser, bone surgery, ablation, hard tissue, osteotomy

1. INTRODUCTION

Nowadays the Er:YAG laser is well established in many clinical applications including skin ablation in dermatology [1], enamel preparation in dentistry [2-5], and bone surgery [6-8]. The main advantages of this laser type are the pulsed operation (pulse duration about 100µs-1ms; pulse energy up to 1J) and the strong absorption by water – the wavelength of the Er:YAG laser 2.94 µm coincides with the main spectral absorption peak – which leads to a highly efficient and precise ablation of soft and hard tissue [9,10]. In contrast to many other lasers the preparation of hard tissue like bone, dentine, or enamel is possible with minimal thermal injury [10-13].

The laser parameters of these flash lamp pumped laser systems are typically pulses energies up to 1 J, pulse repetition rates up to 100Hz, pulse durations of 100µs-1ms, and mean laser powers up to about 20W. As an alternative, actually a novel diode pumped Er:YAG laser system (Pantec Engineering AG) becomes available, with mean laser power up to 30W, pulse energy up to 150mJ, and pulse repetition rate up to 2kHz. For the new system some technical benefits can be expected, e.g. the longer lifetime of the pump source (diode laser) compared to the flash lamp or the realization of more compact and robust laser systems due to the smaller laser cavity [14]. Because high pulse power is a more crucial factor for destruction of optical fibers than repetition rate, also the transmission of high mean power should be beneficial for the diode pumped system.

While bone ablation by flash lamp pumped Er:YAG laser has been investigated in several published studies, there are only first experiments done with the diode pumped Er:YAG laser system [15-17]. These showed a remarkable good

ablation quality and speed in bone cutting but indicate also the need of moistening when using higher mean laser power. The resulting grooves were slightly cone shaped with sharp edges at the surface. However, the groove depth was limited to about 2mm. For some applications the bone structures are thicker and therefore the ablation depth should to be deeper.

Now a new generation of the diode-pumped Er:YAG laser with higher pulse energy and higher mean laser power becomes available. So the aim of the present study is to investigate this new laser system for bone cutting and particularly to find adaptive parameters to increase the cutting depth. At first optical ray tracing simulations were performed in order to design various focusing units and to determine the key parameters (focus diameter, focal length, and numerical aperture). According to the simulation results two focusing units were realized and tested using various irradiation parameters in order to increase the cutting speed.

2. MATERIAL AND METHODS

2.1 Optical ray tracing simulations

At first optical ray tracing simulations (Zemax) were performed in order to design various focusing units and to determine their key parameters (focus diameter, focal length, and numerical aperture). For simulation of the laser beam the out-coming beam diameter of the diode-pumped Er:YAG-laser (DPM-30, high brightness, Pantec Engineering) was measured using a variable aperture in a fixed position. From this the beam divergence was calculated. With this data several lens combinations were simulated and optimized to achieve an almost homogeneous intensity distribution in the focus (top-hat profile).

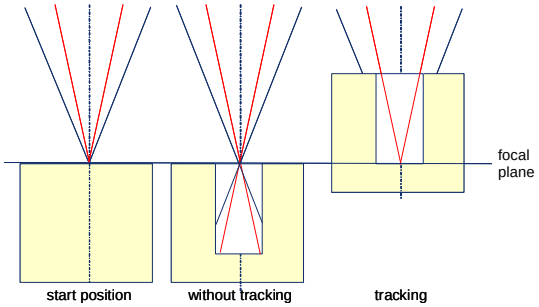

Figure 1. Scheme of different effects occurring while increasing ablation depth without and with axial tracking.

Then two optical designs with 250µm beam diameter and 330µm, respectively, were used to compare focus diameter, focal length, and numerical aperture. In order to get an idea about the decrease of ablation with increasing pulse number, dependent on the laser beam parameter, the expected the laser pulse energy as well as the radiant exposure at the bottom of the increasing groove were calculated. For this an absorbing slit was implemented in Zemax, which simulates the shadowing of the laser beam at the sample surface. The slit width corresponds to expected grove width, which approximately equals the focus diameter . The axial slit position was either fixed or axially moved to compensate for the ablation, modeling an axially fixed or tracked sample position (figure 1).

2.2 Samples

As hard tissue samples we used fresh slices of pig bone, each with 9-10mm thickness, prior stored in water.

2.3 Er:YAG laser system and experimental setup

The principle experimental setup for the preliminary in vitro investigations is shown in figure 2. The used diode pumped Er:YAG laser (DPM-30, High Brightness, Pantec Engineering) provides an adjustable mean laser power up to 25 W, pulse repetition rate 200 Hz – 2 kHz, and pulse duration 10µs – 250µs. We always used a pulse duration of 250µs.

According to the simulation results the laser beam was focused by two lens combinations.

For rinsing the sample surface we provided an appropriate water spray unit (using the handpiece and control unit of a dental Er:YAG laser, KEY2, KaVo), which was positioned behind the last lens. Water flow was 6ml/min according to the results of prior investigations [17]. These investigations showed also that the nozzle position relative to the direction of sample movement influences the thermal injury. Figure 2 show the used nozzle position which leads to minimum thermal effects.

In order to prevent accumulation of water particularly in deeper grooves, an additional nozzle with air flow of 2.4l/min was positioned parallel to the sample surface and directed along the groove.

In front of the distal lens we placed a glass slice (thickness: 170µm) to protect the lenses. The slice was replaced when a transmission loss was detected.

The defined positioning and movement of the samples were realized by a computer controlled linear stage (MICOS, Corvus Eco & 3xLS110) and a special sample holder, which allows to fix the sample surface in a reproducible z-position. In order to ensure a defined radiant exposure (laser energy per area; H), the samples were moved with a constant velocity v during irradiation with various laser parameter.

With help of a computer controlled shutter unit in front of the laser it was possible to reproduce the same procedure for each sample: a) switching the laser on, b) waiting for about 10 seconds to stabilize the laser operation and c) opening the shutter and starting the movement of the sample. After one cycle with a sample movement of typically 10 mm the shutter was closed and the sample stopped.

Before these bone cutting experiments the focus position and depth were determined by irradiation and simultaneous movement of a piece of black photo paper in horizontal and vertical direction. Also prior to each irradiation experiment the laser power was measured (Laserstar, OPHIR) and adjusted. Then the experiment was performed with the particular parameters (diode current / laser power, pulse duration, repetition rate, movement velocity, amount of rinsing).

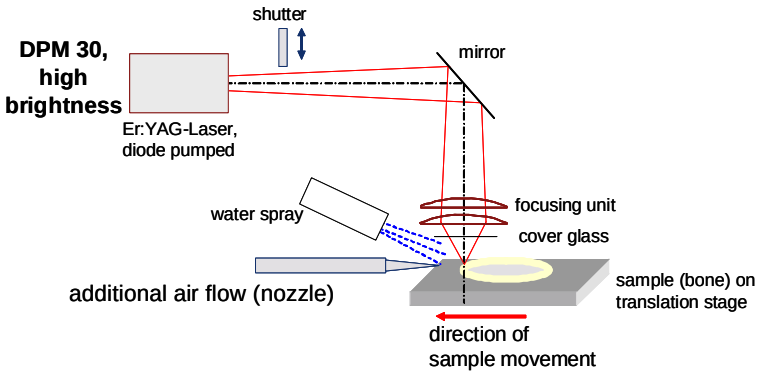

Figure 2. Experimental set-up for irradiation of the samples with defined parameters (prior investigations show improved cooling effect by moving the sample towards the water spray while irradiation [17].

Following investigations were performed:

Experiment 1

A lens combination of a silicon lens (convex/plane, f = 60mm) and a sapphire lens (convex/plane, f = 73mm) was used, with a calculated focus diameter of 250µm.

Laser parameters were: pulse energy EP = 69mJ, v = 200Hz. The movement velocity was 10 mm/s, which corresponds to a number of pulses per position n_{Pos} = 5. According to our experience from prior investigations we expect under this condition a homogeneous cutting.

In sum 9 cycles were performed and after each cycle the groove depth was measured using a light microscope and dial gauge. The sample was axially tracked to position the actual groove bottom in the focal plane before starting the next cycle.

Experiment 2

The idea of experiment 2 was to use a lens combination resulting in a larger focus diameter and smaller NA in order to increase the maximum groove depth. A lens combination of a sapphire lens (convex/plane, f = 100mm) and a silicon lens (convex/plane, f = 60mm) was used, with a calculated focus diameter of 330µm.

Laser parameters were: pulse energy EP = 72.5mJ, v = 200Hz. The movement velocity was 10 mm/s, which corresponds to a number of pulses per position n_{Pos} = 6.6. In sum 13 cycles were performed.

The other parameters and methods correspond to that of experiment 1.

Experiment 3: Influence of the tracking parameters

The idea of experiment 3 was to reduce the axial tracking and with this the enlargement of the groove depth by defocusing of the laser at the sample surface.

In the first test up to cycle 5 (groove depth 2900µm) the sample was axially tracked as in experiment 2. Then the axial tracking parameter per cycle was reduced (100µm), which leads to an axial focus distance to the expected groove bottom of 2100µm before the last cycle.

In another test the tracking was skipped completely, but the focus plane was positioned 2mm below the sample surface.

The same focusing unit and irradiation parameters as in experiment 3 were used. In sum 13 cycles were performed, using the axial tracking parameters of experiment 2 (we skipped the measurement of groove depth after each cycle).

Experiment 4: Influence of the air nozzle

The aim of this experiment was to investigate the need of the additional air nozzle. The same focusing unit and irradiation parameters as in experiment 3, with reduced tracking, were used, but without air nozzle.

2.4 Analysis of the samples

After each irradiation cycle or at the end of irradiation the cuts and grooves were photographed by the help of a light microscope equipped with a digital camera, and the ablation depth (depth of the grooves) was measured.

Following characteristic quantities were calculated using the treatment parameters and the measured ablation depth z:

- the irradiation time per position: $t_M = \varnothing_F / v * n_C$ (1)
- number of pulses per position: $n_{Pos} = t_M * \nu$ (2)
- ablation rate (or ablation speed): $\Delta z / \Delta t = z / t_M$ (3)
- ablation depth per energy: $\Delta z / \Delta E = z / (n_{Pos} * E_P)$ (4)
- ablation per pulse (“precision”) $\Delta z / \text{pulse} = z / n_{Pos}$ (5)
- radiant exposure per pulse H_P: $H_P = E_P / (\pi * r_F^2)$ (6)
- radiant exposure per position H_{Pos}: $H_{Pos} = H_P * n_{Pos}$ (7)
- ablation efficiency $\Delta V / \Delta E$: $\Delta V / \Delta E = z / (n_{Pos} * H_P)$ (8),

with the movement velocity v, beam radius r_F and diameter $\varnothing_F$, the measured ablation depth z, the pulse energy E_P, the laser repetition rate ν, and the number of cycles n_C.

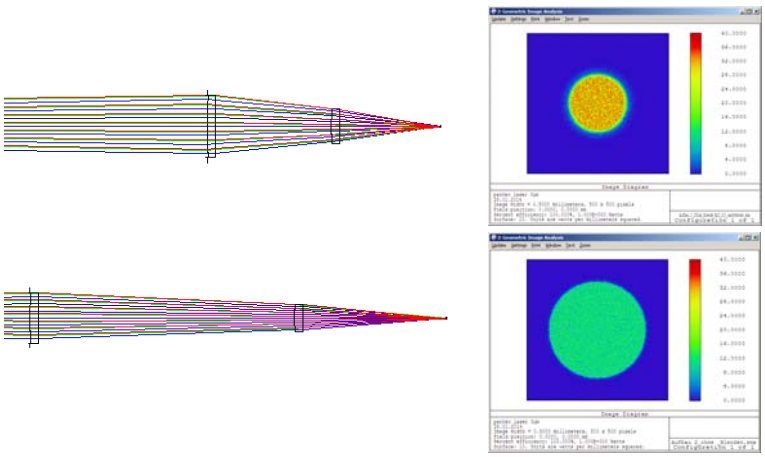

Figure 3. Layout of the optical path and beam profile in focus of the two simulated and optimized lens combinations.

3. RESULTS

3.1 Zemax simulations

Figure 3 shows the optical path and the simulated beam profile in focus of the two simulated and optimized lens combinations, which were also used for the further in vitro investigations. Table 1 comprises the characteristic data of both set-ups. In summary lens combination 1 has a shorter effective focal length and thus a smaller focus diameter, a shorter focus depth at half maximum (FWHM), and a higher NA. Also the spot diagram indicates more aberrations in case of lens combination 1 and with this a slightly worse focus beam profile.

Table 1: Characteristic quantities of the both simulated and optimized lens combinations, used for focussing the laser beam.

	LC1: f_1 = 60mm, f_2 = 73mm	LC2: f_1 = 100mm, f_2 = 60mm
effective focal length / mm	42.3	60.8
focus diameter / µm	250	330
focus depth (FWHM) / mm	1.95	4.52
beam divergence / Numerical Aperture	0.146	0.086

The results of the simulation of the expected radiant exposure at the bottom of groove are depicted in figure 4. If the axial sample position is fixed (left graph), the radiant exposure of lens combination 1 (LC1, 250 µm) is higher compared to lens combination 2 (LC2, 330 µm) up to a groove depth of 1.7mm. Then the radiant exposure of LC2 exceeds more and more the value of LC1. If axial sample position is tracked, then the radiant exposure of LC1 is always higher than LC2 (right graph). Figure 5 shows the simulated losses due to shadowing at the sample surface with increasing groove depth. The increasing energy loss with increasing groove depth is always higher for LC1 than for LC2, regardless of tracking. There are only slight differences between the curves with or without tracking.

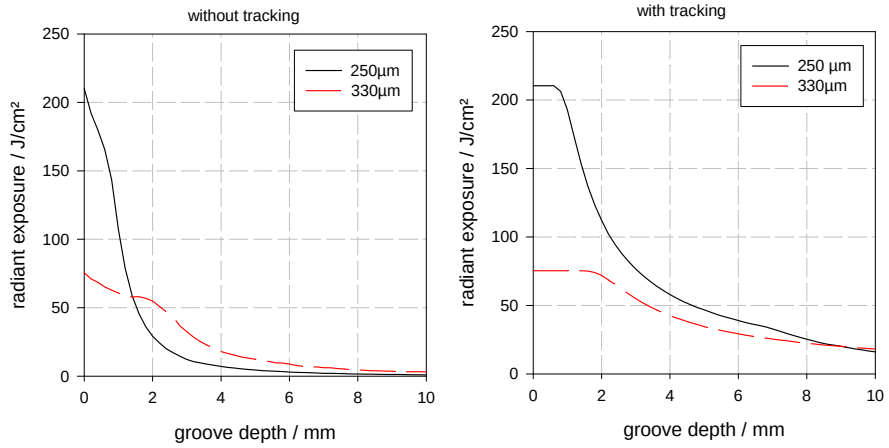

Figure 4. Simulated radiant exposure at the groove bottom for the both investigated lens combinations; left: without axial tracking; right: with tracking.

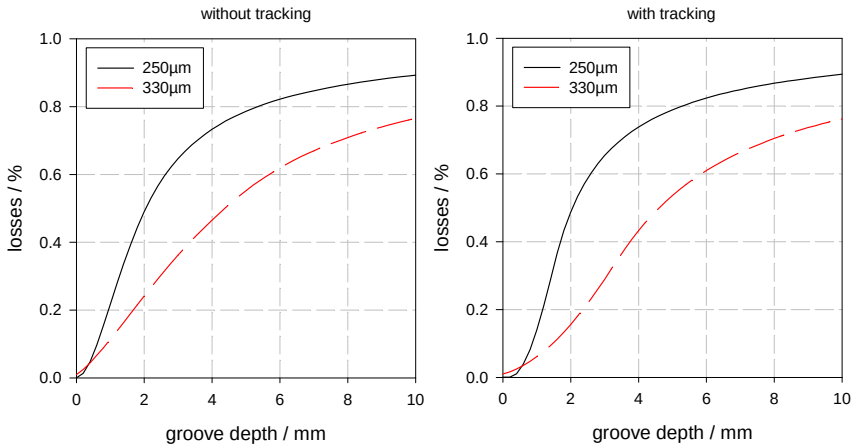

Figure 5. Simulated losses at the groove bottom for the both investigated lens combinations; left: without axial tracking; right: with tracking.

3.2 Experiment 1 and 2

Quality of bone ablation

Figures 6 shows, as an example, some of the resulting grooves in bone using lens combination 1 (focus diameter 250µm) and lens combination 2 (focus diameter 330µm). Up to a cycle number of 4 the grooves have sharp edges and the side view shows a nearly cylindrical shape of the grooves. Then with increasing number of cycles the groove becomes funnel-shaped at the surface, and in this area we detected sometimes a slight browning of the bone, and also sometimes in the deeper region of the grooves.

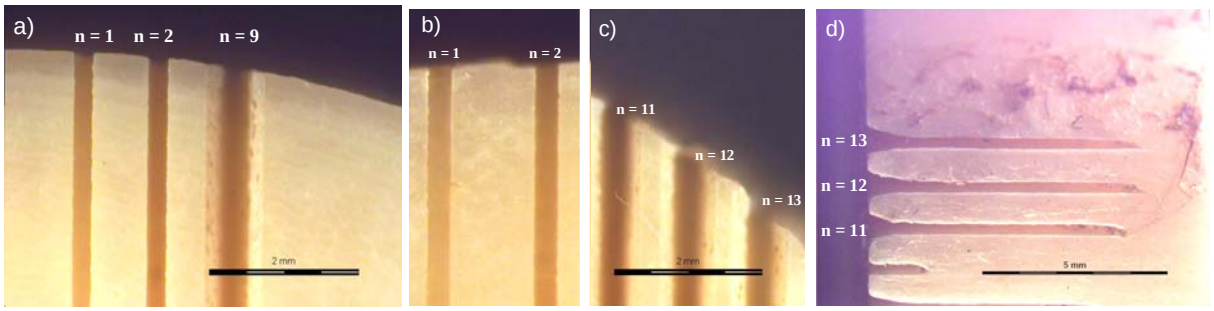

Figure 6. Ablation grooves in a pig bone slice made by diode pumped Er:YAG-laser DPM 30 and with various number n of cycles; a): lens combination 1 / focus diameter 250µm, 69mJ, 200Hz, 10mm/s; b), c), and d): lens combination 2 / focus diameter 330µm, 72.5mJ, 200Hz, 10mm/s; d) is a side view of c).

Geometry of grooves and characteristic quantities

In Figure 7 the measured groove width and depth for the both lens combinations and with increasing number of cycles are depicted. In both cases the groove width increases with increasing number of cycles, but more pronounced for LC1 / focus diameter 250µm. Up to 3 cycles the ablation depth is slightly higher for LC1 than LC2, but for cycles > 3 the groove depth of LC2 exceeds more and more the value of LC1. Table 2 shows the calculated characteristic quantities for 1 cycle and 8 cycles. Both the radiant exposure per pulse H_P and per position H_{pos} are higher for LC1 than for LC2. Also ablation speed and ablation / energy are higher for LC1. But the ablation efficiency is 16% higher for LC2 compared to LC1 for the first cycle and 35% higher for the mean value after 8 cycles.

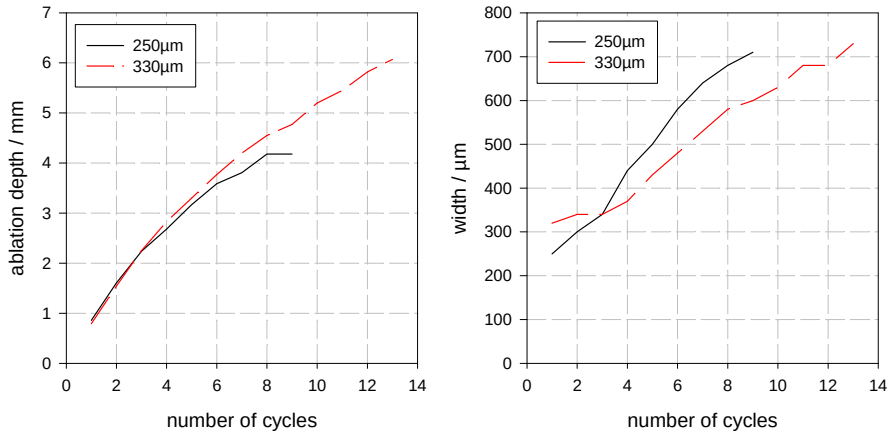

Figure 7. Left: Measured ablation depths at various amount of water (laser parameter: focus diameter 180µm, laser power 2W, 200Hz, movement velocity 2mm/s); right: photomicrographs of the corresponding grooves.

Table 2: Calculated characteristic data according to (1)-(7) for the both lens combinations and the resulted ablation depths in figure 8.

	LC1: 69mJ, 200Hz, **focus diameter 250µm**, 10mm/s		LC2: 72.5mJ, 200Hz, **focus diameter 330µm**, 10mm/s	
number of cycles	1	8	1	8
measured depth	860µm	4180µm	790µm	4550µm
irradiation time per position, t_M	25ms	200ms	33ms	264ms
irradiated pulses per position, n_{pos}	5	40	6.6	52.8
radiant exposure per pulse, H_P	140.5J/cm²		84.8J/cm²	
radiant exposure per position, H_{Pos}	702.7J/cm²	5.62kJ/cm²	559.7J/cm²	4.477kJ/cm²
ablation rate (or ablation speed) $\Delta z / \Delta t$	34.4mm/s	20.9mm/s	23.9mm/s	17.23mm/s
ablation depth per energy, $\Delta z / \Delta E$	2.49mm/J	1.51mm/J	1.65mm/J	1.19mm/J
ablation per pulse ("precision") Δz / pulse	172µm	104.5µm	119.7	86.2µm
ablation efficiency $\Delta V / \Delta E$	0.122mm³/J	0.074mm³/J	0.141mm³/J	0.102mm³/J

3.3 Experiment 3: Influence of the tracking parameters

The reduced tracking leads to a slightly increased ablation depth of 6.1mm compared to 6.07mm in experiment 2 (always axial tracking) and to an obviously reduced funnel-shaped groove at the surface (groove width 520µm compared to 730µm) (grove 1 in figure 8). Without tracking but positioning the focal plane 2mm below the sample surface the resulted ablation depth is 5.63mm (8% less than 6.1mm of exp. 3) and the funnel-shape of the groove is further reduced (width 400µm) (groove 2 in figure 8).

3.4 Experiment 4: Influence of the additional air nozzle

Figure 8 also shows the resulting groove after 13 irradiation cycles with the same parameters as used in experiment 3 (also with reduced tracking) but without the additional air nozzle. There are no differences visible between using the air nozzle or not. Also the ablation depth (6.1mm) is the same value as measured in experiment 3.

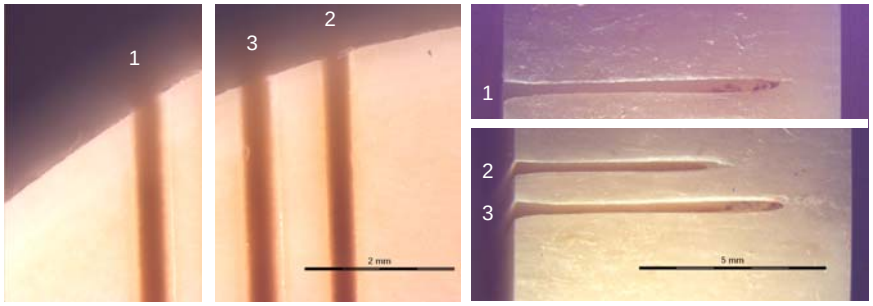

Figure 8. Ablation grooves in a pig bone slice made by diode pumped Er:YAG-laser DPM 30 and with 13 number of cycles; groove 1: reduced tracking; groove 2: without tracking, focus plane is 2mm below the surface; groove 3: without additional air nozzle (lens combination 2 / focus diameter 330µm, 72.5mJ, 200Hz, 10mm/s; the right pictures are side views of the middle and the left pictures.

4. DISCUSSION

By optical ray tracing various lens combinations could be found, which provide well defined beam foci with a homogeneous intensity distribution. The simulated focus diameters correspond very well to the measured groove widths measured at the sample surface for the first couple of cycles. The de facto spatial energy distribution in focus depends on the energy distribution of the actual laser beam. For our simulations we presumed a top-hat profile. The sharp edges of the resulted grooves at the surface support this assumption. The performed optical ray tracing simulations are not only a helpful tool for development of the focusing unit. They can also be used to estimate the influence of treatment parameters, especially the axial tracking, on the expected energy distribution at the surface as well at the groove bottom. Further investigations are planned to compare this values with the measured ablation depths per cycle, depending on the groove depth and the tracking parameters. The idea is to use the simulation for planning the irradiation parameters (focus diameter, NA, movement velocity, tracking parameters) and to pre estimate the resulting ablation geometry.

The presented cutting tests on bone confirm the observed good ablation quality of the prior cutting tests, which were performed with a less powerful laser system (DPM15, Pantec Engineering AG) [17]. Also here the observed ablation quality and precision is remarkable good with sharp edges, nearly perpendicular groove walls, and without visible thermal injury. Now, however, the higher mean laser power and the higher pulse energy result in a significant increase of ablation effect. Especially the maximum measured groove depth (6.1mm, focus diameter 330µm) achieved with the 30W laser system is about three times greater than the values which we achieved with the 15W laser system (about 2mm, focus diameter 220µm).

Regarding the ablation rate the experiments show that up to an ablation depth of about 2mm the smaller focus diameter of LC1 leads to a higher ablation speed and ablation depth per energy compared to the larger focus. This is due to the higher radiant exposure. For deeper cuts the ablation per cycle decreases, more pronounced for the smaller focus diameter. This can be explained by the increase of losses caused by defocusing and shadowing of the laser beam at the sample surface, which is also confirmed by the simulation results (figure 5). Regarding “precision” the calculated ablation depth per pulse is an important characteristic quantity (86.2µm-172mm per pulse; minimum of prior

investigation: 43.2µm [17]). The calculated ablation efficiency is always higher for the larger focus diameter (0.141mm³/J, 1 cycle). It is in the region of published values for Er:YAG lasers (0.067-0.233mm³/J) and higher than values found for CO_2 lasers (0.018-0.04mm³/J) [18-20].

The axial tracking of the sample has also an important influence on the achievable groove geometry, especially the maximum groove depth and the groove width and shape at the surface. Without tracking, but focusing below the bone surface, the groove depth is reduced compared to the results with tracking, but the funnel-shape of the cut at the surface is also reduced. The reason is the fixed beam diameter on the bone surface and the defocusing of the laser beam at the groove bottom, which is also confirmed by the simulation results (figure 4). The slightly increased groove depth and the reduced groove width indicate that reduced tracking seems to be a good compromise between complete and no tracking. Future research will be on the further optimization of tracking, supported by appropriate simulations.

In summary, the high ablation speed on the one hand, and the achievable high "precision" on the other hand indicate the high potential of the diode pumped Er:YAG laser system for precise bone ablation/cutting.

In conclusion, the presented results show a high potential of the diode pumped Er:YAG laser for bone surgery. Especially the novel 30W-system allows fast and deep cutting of bone. The presented preliminary tests are an excellent basis for the development of new applications and devices for bone surgery under use of the diode-pumped Er: YAG laser.

5. ACKNOWLEDGMENTS

The authors wish to thank Pantec Engineering AG for financial support (providing the laser system) and also Andrea Böhmler for preparation of the histological sections.

REFERENCES

[1] Alster, Tina S., and Jason R. Lupton., "Lasers in dermatology.", American journal of clinical dermatology, 2(5), 291-303 (2001)
[2] Van As, G., "Erbium lasers in dentistry", Dental Clinics of North America, 48 (4), 1017-1059 (2004).
[3] Gentil De Moor, R.J., Delme, K.I., "Laser-assisted cavity preparation and adhesion to erbium-lased tooth structure: part 2. present-day adhesion to erbium-lased tooth structure in permanent teeth", The journal of adhesive dentistry, 12 (2), 91-102 (2010).
[4] De Moor, R.J., Delmé, K.I., "Laser-assisted cavity preparation and adhesion to erbium-lased tooth structure: part 1. Laser-assisted cavity preparation", The journal of adhesive dentistry, 11 (6), 427-438 (2009).
[5] Ishikawa, I., Aoki, A., Takasaki, A.A., "Clinical application of erbium:YAG laser in periodontology.", Journal of the International Academy of Periodontology, 10 (1), 22-30 (2008).
[6] Arnoldner, C., Schwab, B., Lenarz, T., "Clinical results after stapedotomy: A comparison between the erbium: Yttrium-aluminum-garnet laser and the conventional technique", Otology and Neurotology, 27, 458-465 (2006)
[7] Nagel, D., "The Er:YAG laser in ear surgery: First clinical results", Lasers Surg.Med., 21, 79-87 (1997)
[8] Parrilla, C., Galli, J., Fetoni, A.R., Rigante, M., Paludetti, G., "Erbium: yttrium-aluminum-garnet laser stapedotomy-A safe technique," Otolaryngology - Head and Neck Surgery, 138, 507-512 (2008)
[9] Hale, G. M., Querry, M. R., "Optical constants of water in the 200-nm to 200-µm wavelength region", Appl. Opt. 12, 555-563 (1973).
[10] Hibst, R., Keller, U., "Experimental studies of the application of the Er:YAG laser on dental hard substances: I. Measurement of the ablation rate", Lasers in Surgery and Medicine, 9 (4), 338-344 (1989).
[11] Keller, U., Hibst, R., "Experimental studies of the application of the Er:YAG laser on dental hard substances: II. Light microscopic and SEM investigations", Lasers in Surgery and Medicine, 9 (4), 345-351 (1989).
[12] Kilinc, E., Roshkind, D.M., Antonson, S.A., Antonson, D.E., Hardigan, P.C., Siegel, S.C., Thomas, J.W., "Thermal safety of Er:YAG and Er,Cr:YSGG lasers in hard tissue removal", Photomedicine and Laser Surgery, 27 (4), 565-570 (2009).
[13] Peavy, G.M., Reinisch, L., Payne, J.T., Venugopalan, V., "Comparison of cortical bone ablations by using infrared laser wavelengths 2.9 to 9.2 µm", Lasers Surg Med., 25(5), 421-34 (1999).
[14] A. Heinrich, C. Hagen, A. Vizhanyo, P. Krammer, S. Summer, S. Gross, C. Böhler, and T. Bragagna, "High power, diode-pumped Er:YAG lasers for soft and hard tissue applications," in Medical Laser Applications and

Laser-Tissue Interactions V, R. Sroka and L. Lilge, eds., Vol. 8092 of Proceedings of SPIE-OSA Biomedical Optics, paper 80921C (2011).
[15] Hagen, C., Heinrich, A., Nussbaumer, B., "High power, diode pumped Er:YAG for dentistry", Lasers in Dentistry XVII. Edited by Rechmann, Peter; Fried, Daniel. Proceedings of the SPIE, Volume 7884, 78840I (2011).
[16] Stock, K.; Hausladen F.; Hibst R., "Investigations on the potential of a novel diode pumped Er:YAG laser system for dental applications", Lasers in Dentistry XVIII. Edited by Rechmann, Peter; Fried, Daniel. Proceedings of the SPIE, Volume 8208, 82080D (2012).
[17] Stock, K., Diebolder, R., Hausladen, F., Wurm, H., Lorenz, S., & Hibst, R., "Primary investigations on the potential of a novel diode pumped Er: YAG laser system for bone surgery", Photonic Therapeutics and Diagnostics IX, Proceedings of the SPIE, Volume 85656, 85656D (2013).
[18] Li, Z., Reinisch, L., Van de Merwe, W.P., "Bone ablation with Er:YAG and CO2 laser: Study of thermal and acoustic effects", Lasers Surg Med., 12(1), 79-85 (1992).
[19] Stanislawki, M., Meister, J., Mitra, T., Ivanenko, M.M., Zanger, K., Hering, P., "Hard tissue ablation with a free running Er:YAG and a Q-switched CO2 laser: A comparative study", Appl Phy B., 72(1), 115-20 (2001).
[20] Ivanenko, M.M., Hering, P., "Hard tissue ablation with a mechanically Q-switched CO2 laser", Proc SPIE Int Soc Opt Eng., 3565:110-5 (1999).